VIII International Conference on Computational Methods in Marine Engineering
MARINE 2019
R. Bensow and J. Ringsberg (Eds)

TO EVALUATE THE INFLUENCE OF DOF ON MANOEUVRING PREDICTIONS BY DIRECT CFD ZIG-ZAG SIMULATIONS

XIN GAO* AND GANBO DENG†

* Dynamics of Maritime Systems (DMS)
Technical University of Berlin
SG 17, Salzufer 17-19, 10587 Berlin, Germany
e-mail: x.gao@campus.tu-berlin.de, www.dms.tu-berlin.de

† Laboratoire de recherche en Hydrodynamique, Énergétique et Environnement Atmosphérique (LHEEA)
Ecole Centrale de Nantes
1 Rue de la Noë, B.P. 92101, 44321 Nantes Cedex 3, France
email: ganbo.deng@ec-nantes.fr, lheea.ec-nantes.fr

Key words: DOF, Manoeuvring Predictions, Zig-Zag, CFD, Direct Manoeuvring Simulations

Abstract: *In this paper, direct CFD zig-zag simulations of 10°/10° and 20°/20° are performed in deep water condition under the consideration of different degrees of freedom, namely 3 DOF, 4 DOF, and 6 DOF, to evaluate their influence on manoeuvring predictions. A modern container ship KCS with a slightly simplified semi-balanced rudder is chosen as the benchmark model. All simulations are conducted in the numerical environment FINE™/Marine with the ISIS-CFD code as the flow solver. It solves impressible unsteady RANS equations in full hexahedral unstructured meshes and implicitly couples the flow field with motion equations of a rigid body in 6 DOF. Current direct manoeuvring simulations are achieved by means of the overlapping grid technique. To reduce the computational effort, propeller effect is modelled by a simple prescribed body force model. Trajectories are straightforward recorded without any further treatment to extract hydrodynamic derivatives. The prediction accuracy is evaluated by comparing derived parameters, i.e. overshoot angles and times, peak yaw rates, drift angles, etc. against experimental data. In conclusion, 4 DOF and 6 DOF concept present similar results for current ship type. The tiny changes in pitch and heave motion indicate they can be neglectable to simplify the complex mesh strategy. In addition, the large roll angle over zig-zag manoeuvres implies that 4 DOF concept should be more reasonable for container ships to obtain roll-motion-related data. Meanwhile, 3 DOF concept underestimates all overshoot angles in each simulation. This also highlights the reasonability of 4 DOF concept.*

1 INTRODUCTION

Recently, major liner companies are speeding up to place orders of Mega Container Ships (MCS) with the capacity over 20,000 TEUs so as to provide a more competitive freight rate. For instance, CMA CGM has ordered a group of nine container carriers with each capacity of 22,000 TEUs [16]. However, this type of vessel is usually characterised by 400 metres long and 60 metres wide, which in turn can challenge ship manoeuvrability, especially in the heavy

traffic areas. Conventional CFD manoeuvring predictions are subjected to 3 DOF or 4 DOF considering the complexity of mesh strategy during ship motion and the possibility of introducing numerical error. Whether full 6 DOF can contribute to increasing the prediction accuracy for container ships is still rarely studied. This paper is proposed to evaluate this influence to obtain the accurate results at the lowest expense in the future.

With the development of computer performance and the advance in numerical technique, CFD approach is widely adopted in marine hydrodynamics. For cases like resistance and propulsion, high-fidelity simulations have been achieved without any problems. And, above all, more local flow information can be captured for anytime and anywhere in simulations, which is not available or costly in physical experiments. Considering these advantages, CFD approach is employed in the framework of this paper. As in real experiments, two possible kinds of manoeuvring tests are achievable in use of numerical environment, namely virtual captive model tests (VCMT) and virtual free-running model tests (VFRMT). According to the conclusions of successive SIMMAN workshops (2008 and 2014), VCMT has been a suitable alternative to model experiments to perform manoeuvring predictions [10]. Presentative work includes [3, 5, 9, 13, 14]. However, large numbers of simulations and post-processing to extract hydrodynamic derivatives are still inevitable. Combing these derivatives with mathematical models, trajectories can only be predicted. In contrast, the trajectories can be directly recorded to calculate the derived kinematic parameters in VFRMT, as used in the current study. In general, appropriate treatment of propeller and movable rudder are two key points to perform VFRMT. In case of simulating real propeller, time consumption still cannot be affordable for industrial applications, since temporal discretisation must be small enough to solve the propeller rotation. In contrast, propeller effect can be modelled by a body force model to reduce computation effort. On the other hand, the movement of rudder can be realised by different mesh strategies depending on rudder configurations. For highly complex semi-balanced rudder, overlapping grid technique is the only solution for now. Worldwide, several research groups have carried out this type of simulation. Jensen, Klemt, & Xing-Kaeding achieved the turning circle tests using commercial code COMET [7]. The deflection of a simple spade rudder was realised by the sliding mesh technique and the propeller effect is modelled by a body force model. Direct manoeuvring simulations of turning circle tests show reasonable results for yaw rate, tactical diameter, and heel angle. Carrica, Ismail, Hyman, Bhushan, & Stern presented direct free-running manoeuvres for a surface combatant at both model and full scale using in-house code CFD Ship-Iowa V4 packaged with overset grid capability [2]. Dynamic rudder deflection is coupled with ship 6 DOF motion. The results demonstrated the feasibility of VFRMT using overset grid technique, although inaccurate body force model caused some discrepancies. Furthermore, Dubbioso, Durante, & Broglia simulated zig-zag manoeuvres of a tanker-like vessel by means of a global second order accurate finite volume solver Xnavis implemented with overlapping grids on block-structured meshes [4]. Numerical results of zig-zag manoeuvres taking into account different propeller models were compared with the data of free-running model tests. The effect of rudder rate was also investigated. It is concluded that the improvement of a simplified propeller model would be necessary. In another study, by implementing dynamic overset grids into the open source code OpenFOAM, Shen, Wan, & Carrica achieved direct simulations of standard zigzag 10°/10° and modified 15°/1° manoeuvres using the HSVA KCS model [12]. This implementation relied on the library Suggar++ to compute the domain connectivity information (DCI) dynamically at run time. Although numerical results agreed

well with experimental results, each simulation was still subject to months of computation time.

2 NUMMERICAL FRAMEWORK

Numerical simulations are performed in the FINETM/Marine environment, which includes all necessary CFD tools to solve maritime dedicated applications. Non-conformal body-fitted full hexahedral unstructured meshes can be generated by the mesh generation tool HEXPRESS^{TM} on any complex arbitrary geometries. Its flow solver is built on the widespread ISIS-CFD code developed by METHRIC group of ECN. The code solves incompressible unsteady Reynolds-averaged Navier Stokes equations and is also in couple with the motion equations of rigid body. The spatial discretization of transport equations is based on the finite volume method. The velocity field is calculated from the momentum conservation equations, while the pressure field is obtained from the pressure equation (Poisson equation). To solve turbulent flow, several sophisticated turbulence models such as one-equation model (Spalart-Allmaras), two-equation model (Wilcox or Menter), and etc. are available to choose. The turbulence variables can be solved in a form similar to that of the momentum equations. This solution concept also applies to the calculation of each volume fraction of fluid in case of simulating multiphase flow. A detailed numerical implementation of ISIS-CFD code can be found in [11].

3 TEST DISCRIPTION

3.1 Ship model

The ship model selected for the current study is a modern container ship with the name of Korean Container Ship (KCS). Figure 1 shows a 3D overview of this model. It is one of three benchmark ship types used in the SIMMAN 2008 and 2014 workshop. Free-running model tests are newly repeated for SIMMAN 2014 in MARIN. These experimental data with the model scale of 37.89 are used to validate current numerical simulations [8]. In Table 1, necessary main characteristics of ship, rudder, and propeller are listed in model scale as reference [1]. Since the real geometry of ship model in the experiment is not known before current simulations, the head box is retained as the ship model used in SIMMAN 2008 for free-running model tests. The ship is configured with a complicated semi-balanced rudder. Its turning rate is 14.3 deg/s. Since the propeller effect is modelled by an actuator disk, only several geometric parameters are needed. To reproduce original physical experiments, direct manoeuvring simulations are restarted from previous self-propulsion computations at a constant advancing speed of 2.005 m/s.

3.2 Computational mesh

As we know, a high-quality mesh is the basis of accurate numerical simulations. For the current study, there are mainly two challenges. The first one is how to solve the large amplitude roll motion during zig-zag manoeuvres, since almost 17 degrees of roll angle were observed in physical tests. Considering possible numerical errors, the mesh should have the ability to handle the roll angle of at least 20 degrees. According to the state of the art, three mesh strategies are available to deal with this large amplitude roll motion, namely mesh

morphing, sliding mesh and overset grid. However, mesh morphing can lead to a number of negative-volume meshes at around the moment of maximal roll angle, while sliding mesh can capture at most 5 DOF motions without pitch. In view of the possibility to expand to all 6 DOF motions, the overset grid strategy is a suitable selection to further study. Usually, three domains are necessary to implement this strategy, namely background domain, ship domain, and rudder domain. The dimensions of each domain in current study are illustrated in Figure 2, whereby L_{PP} and L_R are the ship length between perpendiculars and the maximal chord line of rudder profile. Ship domain has 4.6 million cells, while background domain and rudder domain have 0.9 million cells and 1.8 million cells, respectively. Totally, 7.4 million cells are used for medium mesh. A comprehensive convergence study including grid size and time step can be found in [6].

Figure 1: 3D overview of KCS model

Table 1: Main characteristics of ship and its appendages

Ship	**Model Scale**	**Ship**	**Model Scale**
L_{PP} [m]	6.0702	I_{XX}/B [-]	0.4000
B_{WL} [m]	0.8498	I_{ZZ}/L_{PP} [-]	0.2500
T [m]	0.2850	**Rudder**	
S_{Ship} [m^2]	6.6381	S_{Rudder} [m^2]	0.0801
LCG [m]	2.9450	**Propeller**	
KG [m]	0.3785	$D_{Propeller}$ [m]	0.2080
GM_T [m]	0.0160	$D_{Hub}/D_{Propeller}$ [-]	0.1860

The second challenge is how to guarantee enough overlapping meshes across the 2mm gap between the moveable rudder blade and the fixed rudder horn. Based on the experience, at least 8 cells in three coordinate directions from each overlapping domain should be generated

to fill this gap to avoid orphan cells. In addition, to ensure a smooth transformation of fluid information, mesh sizes across overset interfaces from different domains should be kept consistent. To reduce the total number of cells and keep the effective rudder force unchanged. The original gap is enlarged twice the size by reducing the area of the rudder horn, while the rudder blade remains unchanged. In Figure 3, a mesh configuration near the rudder using medium mesh is demonstrated. A prescribed refinement box within the range of rudder execution is proposed to guarantee a successful overset interpolation, however, with many more cells. An alternative to achieve accurate overset interpolation is by adaptive grid refinement (AGR), which can automatically refine the mesh during the computation and meanwhile smooth out the transition in cell sizes across overset interfaces between domains. Some applications can be found in [15].

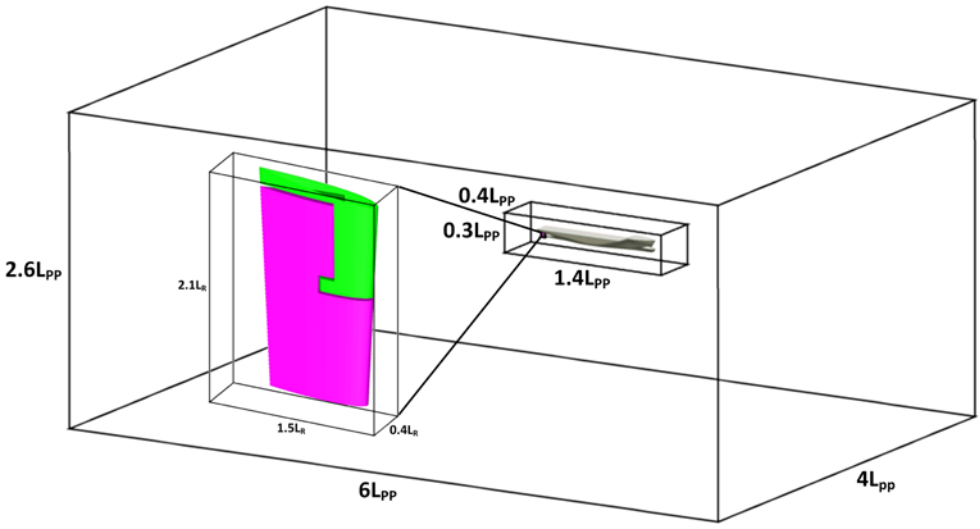

Figure 2: Dimensions of three-domains configuration

3.3 Computational settings

The final zig-zag simulation is set as an unsteady simulation. Robust turbulence model *k-ω* SST is used to close RANS equations. Free surface is solved by means of VOF method with a high-resolution scheme BRICS. It cannot only guarantee a sharp interface between two fluids but also can avoid the limit of courant number. The boundary conditions are illustrated in Figure 4. For inlet, outlet and side patches, far field condition is used. A Dirichlet or a Neuman condition can be alternately applied depending on the local flow direction. Prescribed pressure condition (Dirichlet condition) is adopted for top and bottom patches, on which the pressure value can be updated according to the free surface position. On the ship hull and the rudder surface, wall function is used to solve the flow near the solid patches without extremely fine mesh. Furthermore, slip wall condition is set on deck because we are not interested in it. The external patches of ship domain and rudder domain are defined as overset boundary condition, on which the flow solver allows the information exchange across different domains.

Direct manoeuvring simulation is restarted from a previous converged self-propulsion test at a constant advancing speed. For 3 DOF and 4 DOF concept, pitch and heave motion in the self-propulsion test are blocked, while they are free to be solved for 6 DOF concept. In the 3 DOF manoeuvring simulation, only planar DOFs (namely surge, sway, and yaw motions) are free. The additional free motion in the 4 DOF simulation is the roll motion, while all motions are free in the 6 DOF simulation. The rudder motion is controlled by a compiled FORTRAN library, which can be edited according different steering pre-settings. During the unsteady manoeuvring motion, background domain has only planar motion, in contrast, body fitted overset grid is extended to perform roll, pitch, and heave motion. The propeller effect is

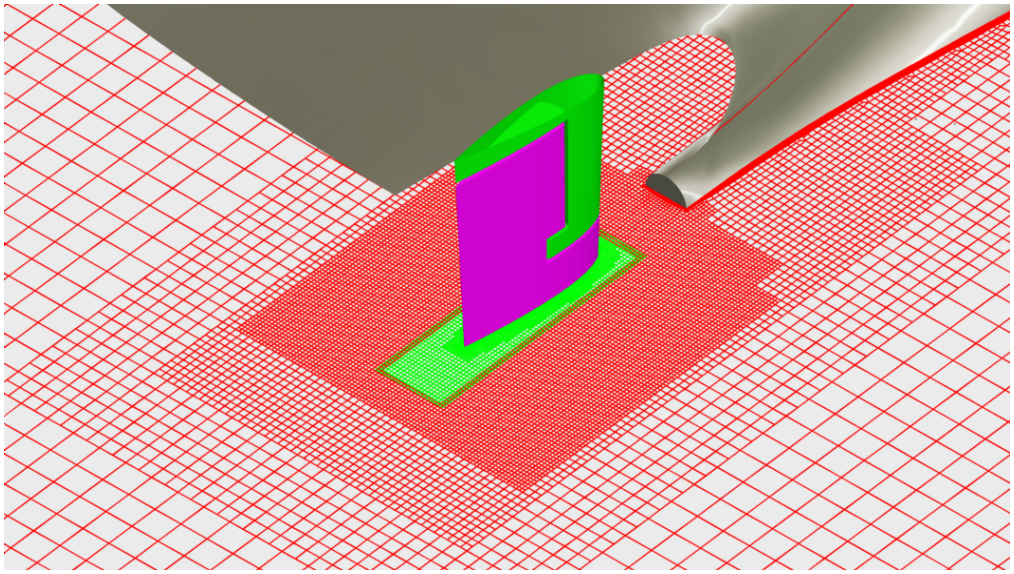

Figure 3: Medium mesh configuration near the rudder

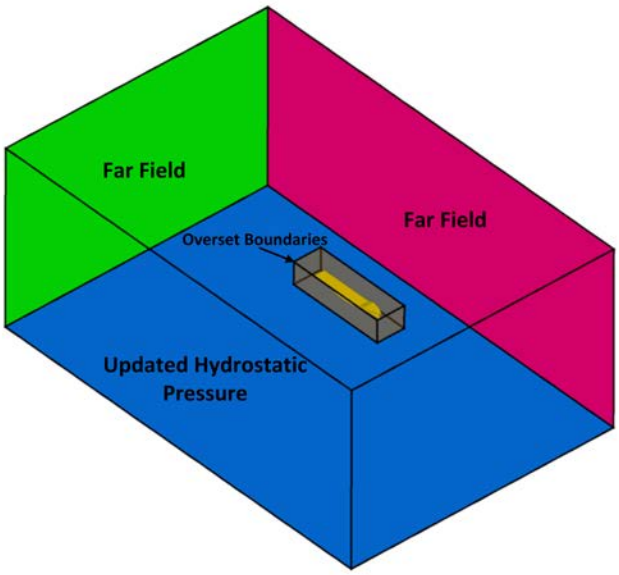

Figure 4: Boundary conditions in the framework of current study

modelled by an actuator disk. It updates the thrust in accordance with a given KCS open water curve measured in Korea Research Institute of Ships and Ocean Engineering (KRISO) for current study. To ensure a precise propeller force, the update procedure is called at each time step. The convection term of the transport equation to solve volume fraction is discretized by BRICS scheme, while AVLSMART scheme is employed for the discretization of convection terms of other transport equations. 10 non-linear iterations are given to proceed the outer loop of iterative algorithm. A pre-conditioned biconjugate gradient stabilized method named PCGSTAB_MB is adopted to solve equation systems. According to the convergence study of time step, 0.02 second is a trade-off value between accuracy and efficiency [6]. Trajectories are recorded in inertial system, whose origin corresponds to the middle point of L_{PP} at the initial time. The details of discretisation scheme and solution algorithm are also explained in [11]

4 RESULTS AND DISCUSSIONS

Direct manoeuvring simulations are performed on three nodes in the cluster of the department of dynamic systems at the technical university of Berlin. Totally, 64 processors are used for each simulation. With the help of the efficient actuator disk, a 4 DOF zig-zag simulation in deep water condition with 7.4 million cells took only 3 days. Taking into of a previous self-propulsion simulation, 4 days are still acceptable. For 3 DOF and 4 DOF concepts, the model self-propulsion point (MSPP) is equal to 11.3 rps, which is only 2.1% lower than the experimental value of 11.50 rps provided by MARIN. For 6 DOF concept, this value stays almost the same as the revolution rate in the experiment. In Figure 5 and Figure 6, numerical results for cases of zig-zag 10°/10° and 20°/20° to starboard using different DOF concepts are compared with the experimental data published in SIMMAN 2014. To ensure the credibility of numerical simulations, validation and verification procedures are conducted for 3 DOF and 4 DOF concept under the consideration of gird size and time step. Space constraints permit only the comparison of kinematic parameters in different DOFs to be discussed. Interested readers can refer to [6].

Since the International Maritime Organization (IMO) has only specified the criteria to evaluate ship yaw-checking ability up to the second overshoot angle, all current simulations are shut down shortly after the second peak heading to save computational time. The kinematic parameters to be discussed in Figure 5 and 6 include heading Ψ, rudder angle δ, drift angle β, roll angle ϕ, resultant velocity V, pitch angle θ, vertical displacement ζ, and dimensionless yaw rate r' and roll rate p'. As can be seen in Figure 5, the results of 4 DOF concept are almost in accordance with that of 6 DOF concept, e.g. yaw angle, yaw rate, drift angle, etc. Additionally, the results for each concept agree very well with experiment data before the second rudder execution. And except for roll-motion-related parameters, 3 DOF concept can also have a good agreement with experimental values as illustrated from Figure 5.1 to Figure 5.4. Especially, the difference of the first overshoot angle between the numerical result and the experimental value is only 2 degrees, while these values are 3.3 degrees and 3.2 degrees for 4 DOF and 6 DOF concept. The value of the difference of the second overshoot angle for 3 DOF concept remains the same with 4 DOF (or 6 DOF) concept, however, in opposite signs. Despite of this good agreement, 3 DOF concept cannot provide roll-motion related information, which can be important for mega container ships. Figure 5.5 and 5.6 provide these interesting data regarding roll angle and roll rate for 4 DOF and 6 DOF concept

and experimental data. The numerical results show the similar trends to change as the data of the experiment. The first peak roll angle is well predicted, while the second numerical roll angle is 2 degrees and 1 degree larger than experimental value for 4 DOF and 6 DOF concept. The roll rate also agrees well with experimental data for 4 DOF and 6 DOF concept. However, after the third rudder execution there is a phase shift. Because of the limited experimental data, no pitch and heave relevant data are available for now. Therefore, only numerical results are exhibited here. In fact, the pitch and heave motion in Figure 5.7 and 5.8 have a tiny change over manoeuvring motions. The pitch amplitude is only 0.2 degree and the heave amplitude is merely 0.007m. This means they can be neglected for current situation. Concerning the resultant velocity in Figure 5.4, the value rises at the beginning of the zig-zag motion in the experiment (see thick red line), which is impossible with the setup used in the CFD. This phenomenon may due to the procedure employed in the experiment. In current simulation, the computation before the zig-zag motion is a captive motion with zero rudder angle and yaw angle, while in the experiment, a counter ruder must be given because of the asymmetric inflow to the rudder. Hence, there may be some experiment uncertainties with respect to the first overshoot angle.

Figure 6 depicts the results of zig-zag 20°/20° simulations and corresponding experimental data. It is similar to zig-zag 10°/10° simulations, all variables for 6 DOF concept have the same changing trends as for 4 DOF concept. The agreements of kinematic variables between the 3 DOF concept and the experiment shown from Figure 6.1 to Figure 6.4 are still quite good. Nevertheless, the disadvantage of 3 DOF concept to predict roll motion highlights the necessity to increase the number of DOF. Furthermore, in zig-zag 20°/20° simulations 3 DOF concept underestimates both overshoot angles with 6.5 degrees and 5.5 degrees. While 4 DOF and 6 DOF have the same discrepancy of the first overshoot angle for 2.1 degrees, the discrepancy of the second overshoot angle for 6 DOF concept is only 1.2 degrees, which is better than 4 DOF concept for 4.7 degrees. In Figure 6.4, 3 DOF and 6 DOF concept can give identically accurate speed loss, but 4 DOF concept shows a large discrepancy of the lowest speed loss for about 0.1 m/s compared with the experimental value. In terms of roll angle and roll rate, 6 DOF concept presents a better prediction than 4 DOF concept. The peak roll angles for 6 DOF concept keep the same value with the experimental values despite of time shift for the second peak value. 6 DOF concept is also apparently better than 4 DOF concept for roll rate, especially after the third rudder execution 4 DOF concept underestimates the dimensionless roll rate for 0.1. Besides, the time shift still exists. The pitch and heave motion in this case are still quite tiny. The amplitude of pitch and heave motion is 0.36 degree and 0.012 m, respectively, which also means these two degrees of freedom can be neglectable for current simulation condition.

As can be seen from Figure 5.5 and 6.5, the object ship suffers from a significant roll motion during manoeuvres. Comparing Figure 5.5 with 5.1 or Figure 6.5 with 6.1, it is clear that the time of peak roll angle does not correspond with the time of peak yaw angle, but with the rudder execution. The maximal roll angle happens when or shortly after the rudder reaches the counter target angle. As an example, Figure 7 illustrates the contours of midship plotted by axial vorticity ω_x at the moment of two peak roll angles for zig-zag 10°/10° in 4 DOF. When the ship is subjected to the peak roll angle inwards, the flow around outward bilge has an obvious separation. This vortex structure caused by the roll motion can change the distribution of hydrodynamic forces, which can then influence the ship manoeuvrability.

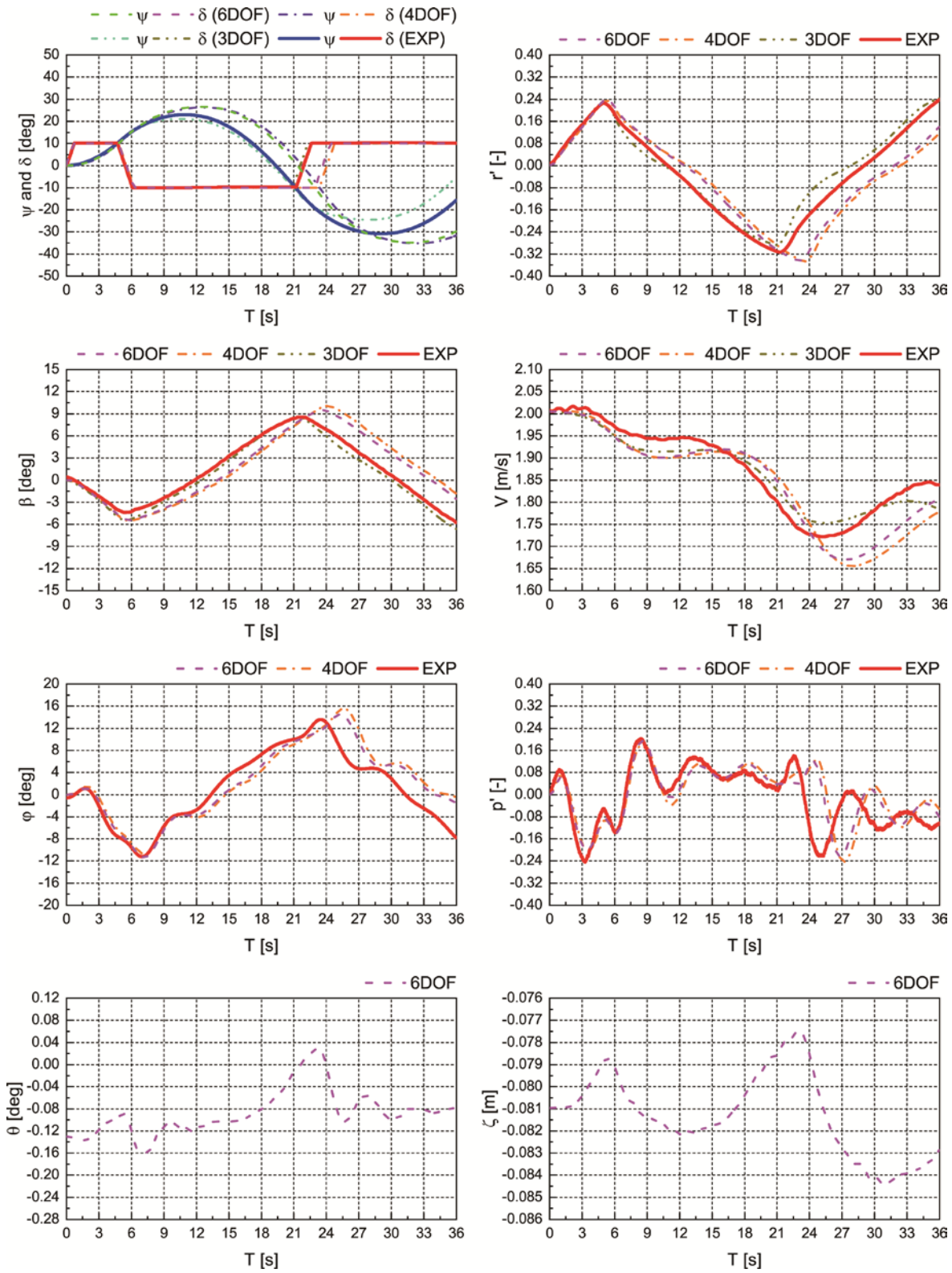

Figure 5: Comparison of kinematic parameters for zig-zag 10°/10° to starboard in different DOF concepts (Top left: 5.1, Top right: 5.2, Bottom left: 5.7, Bottom right: 5.8)

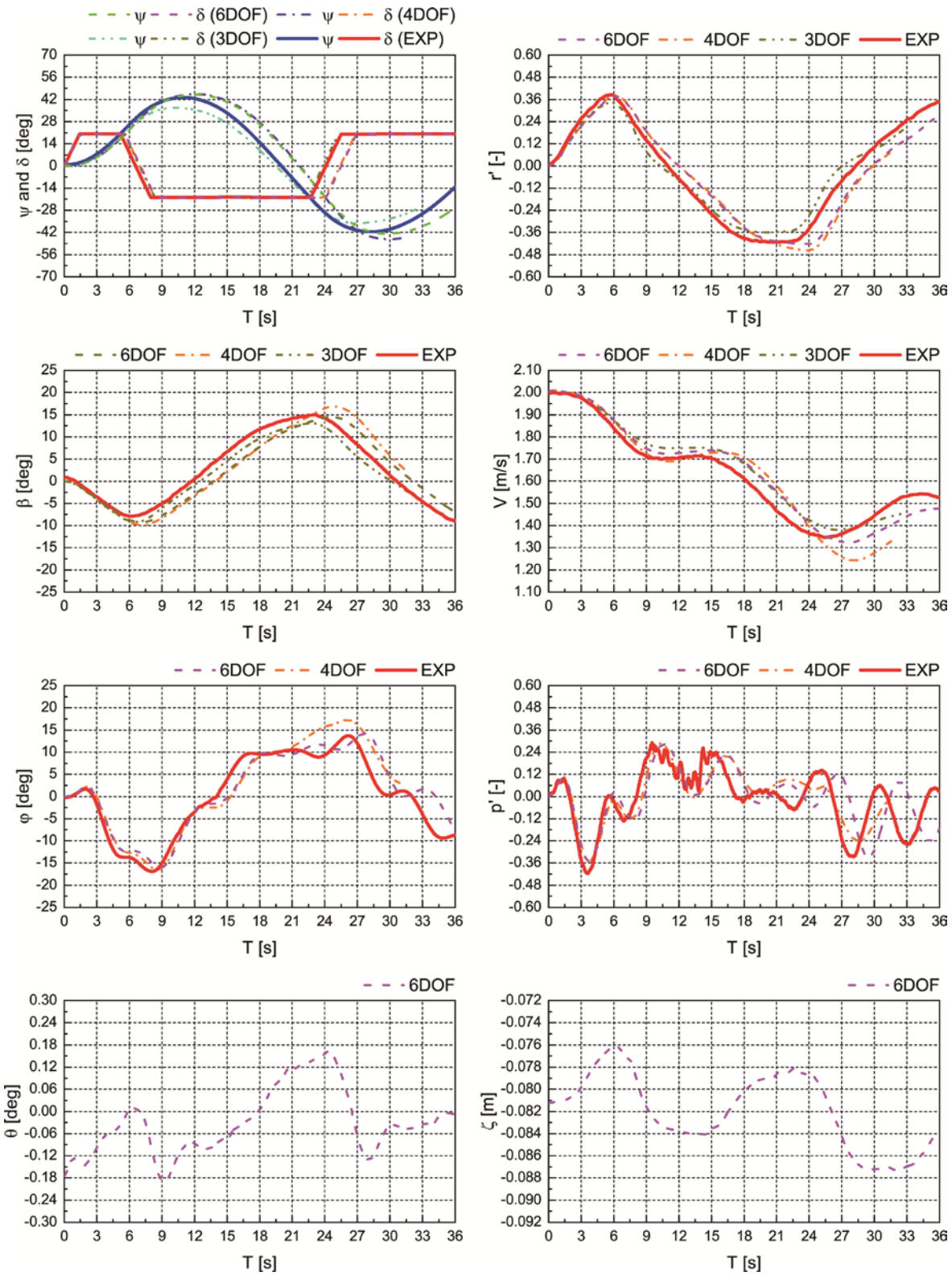

Figure 6: Comparison of kinematic parameters for zig-zag 20°/20° to starboard in different DOF concepts (Top left: 6.1, Top right: 6.2, Bottom left: 6.7, Bottom right: 6.8)

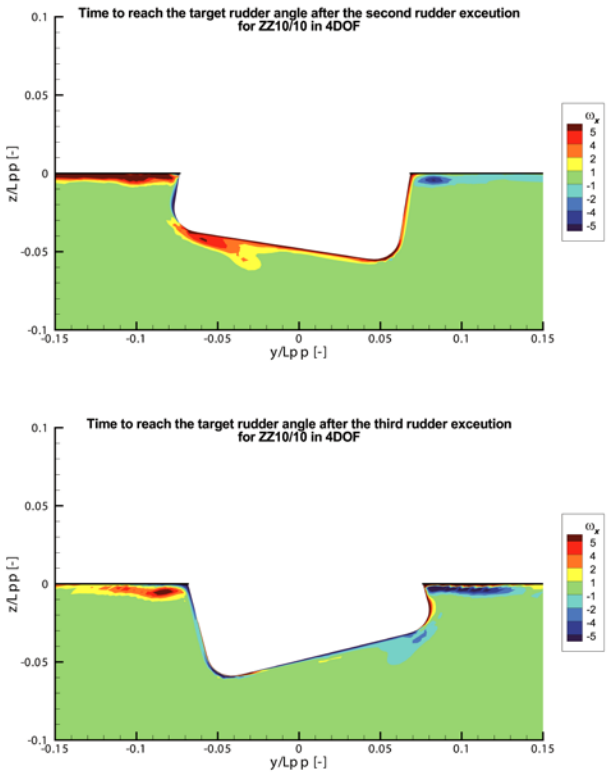

Figure 7: Contours of vortex structure amidships for zig-zag 10°/10° in 4 DOF (See from bow to aft)

5 CONCLUSIONS

From the simulations that have been performed, it is possible to conclude that 4 DOF concept can be more reasonable than 6 DOF concept for current ship type since the tiny pitch and heave motion observed in the simulations can be neglected. As a result, mesh strategy can be simplified using 4 DOF concept. Additionally, large roll angle during manoeuvring motions implies that 4 DOF concept should be preferred to the container ships which may have severe roll motion in service. Compared with 4 DOF and 6 DOF concept, 3 DOF concept underestimates all overshoot angles of each simulation. The reason for above mentioned behaviour can be explained by the change of the side projected area under the waterplane in different DOFs, which indirectly affects the distribution of hydrodynamic forces and moments.

6 ACKNOWLEDGEMENTS

The authors would like to thank the engineering office of NUMECA in Germany for its license and also the technical staff in the department of DMS for HPC resource to implement the study. Additionally, fruitful discussions over simulations with Professor Cura Hochbaum and Dr. Uharek are gratefully acknowledged. At last, the authors would like to extend their thanks to MARIN for providing the experimental data, especially to Mr. Quadvlieg and Mr. Tonelli. Part of this work was granted access to the HPC resources of [CINES/IDRIS] under the allocation 2018-A0052A01308 made by GENCI.

REFERENCES

[1] Carrica, P. M., Ismail, F., Hyman, M., Bhushan, S., & Stern, F. (2008). *Turn and zigzag maneuvers of a surface combatant using a URANS approach with dynamic overset grids*. Paper presented at the SIMMAN 2008, Copenhagen, Denmark.

[2] Cura Hochbaum, A. (1998). *Computation of the turbulent flow around a ship model in steady turn and in steady oblique motion*. Paper presented at the 22nd Symposium on Naval Hydrodynamics, Washington, D.C., United States.

[3] Dubbioso, G., Durante, D., & Broglia, R. (2013). *Zig-zag maneuver simulation by CFD for tanker like vessel*. Paper presented at the 5th International Conference on Computational Methods in Marine Engineering, Hamburg, Germany.

[4] El Moctar, O. M. (2001). Numerical computations of flow forces in ship manoeuvring. *Ship Technology Research, 48*(3), 98-123.

[5] Gao, X. (2019). *Analysis of the influence of bilge keels on manoeuvring by means of virtual zigzag tests.* (M.Sc.), Technical University of Berlin,

[6] Jensen, G., Klemt, M., & Xing-Kaeding, Y. (2004). *On the way to the numerical basin for seakeeping and manoeuvring*. Paper presented at the 9th Symposium on Practical Design of Ship and Other Floating Structures, Luebeck Travemuende, Germany.

[7] MARIN. (2010). Manoeuvring tests on KCS. *MARIN Report: 23991-1-SMB*.

[8] Ohmori, T., & Miyata, H. (1993). Oblique Tow Simulation by a Finite-Volume Method. *Journal of the Society of Naval Architects of Japan, 1993*(173), 27-34.

[9] Quadvlieg, F., Stern, F., Simonsen, C. D., & Otzen, J. F. (2014). *Proceedings of SIMMAN 2014*, Copenhagen, Denmark.

[10] Queutey, P., & Visonneau, M. (2007). An interface capturing method for free-surface hydrodynamic flows. *Computers & fluids, 36*(9), 1481-1510.

[11] Shen, Z. R., Wan, D. C., & Carrica, P. M. (2015). Dynamic overset grids in OpenFOAM with application to KCS self-propulsion and maneuvering. *Ocean Engineering, 108*, 287-306.

[12] SIMMAN 2014. (2014). Retrieved from https://simman2014.dk

[13] Simonsen, C. D., & Stern, F. (2005). RANS maneuvering simulation of Esso Osaka with rudder and a body-force propeller. *Journal of Ship Research, 49*(2), 98-120.

[14] Toxopeus, S. L. (2011). *Practical application of viscous-flow calculations for the simulation of manoeuvring ships.* (Ph.D.), Delft University of Technology,

[15] Wackers, J., Deng, G., Leroyer, A., Queutey, P., & Visonneau, M. (2012). Adaptive grid refinement for hydrodynamic flows. *Computers & fluids, 55*, 85-100.

[16] World Maritime News Staff. (2018). Steel Cut for CMA CGM' s 22,000 TEU Behemoths, World' s Largest Boxships. Retrieved from https://worldmaritimenews.com/archives/257983/steel-cut-for-cmacgms-22000-teu-behemoths-worlds-largest-boxships